

# Study of quantum Otto heat engine using driven-dissipative Schrödinger equation

You-wei Fang,<sup>1</sup> Yu-ting Zheng<sup>1</sup> and Jun Chang<sup>1,\*</sup>

<sup>1</sup>*College of Physics and Information Technology,  
Shaanxi Normal University, Xi'an 710119, China*

(Dated: October 13, 2020)

The quantum heat engines have drawn much attention due to miniaturization of devices recently. We study the dynamics of the quantum Otto heat engine using the driven-dissipative Schrödinger equation. Starting from different initial states, we simulate the time evolutions of the internal energy, von Neumann entropy, power and heat-work conversion efficiency. The initial state impacts on these thermodynamic quantities before the Otto cycle reaches stable. In the transition period, the efficiency and power may be higher or lower than the corresponding values in the cyclostationary state. Remarkably, the efficiency could surpass the Otto limit and even the Carnot limit. Thus, we suggest that periodically pumping could improve the performance of quantum heat engines. Furthermore, we propose a new quantum engine working in a single reservoir to convert the pump energy into mechanical work. This manipulative engine could potentially be applied to working in the microenvironments without a large temperature difference, such as the biological tissues in vivo. Our protocol is expected to model a new quantum engine with the advantage of applicability and controllability.

## I. INTRODUCTION

Converting heat into mechanical work periodically, the heat engines as the generators of motion triggered both the industrial revolution and the theoretical development of thermodynamics in the 18th and 19th centuries. Recently, the heat engines have been re-invigorated by miniaturization of devices [1]. Experimentally, elaborate efforts have been made on the design of the machines employing quantum systems, such as harmonic oscillators [2], ultracold atoms [3], a single particle, such as an atom, ion, electron [4–8] and molecule [9, 10] as well as a spin-1/2 system [8, 11–13] and qubit system [14–16]. They work at the atom level to convert heat or light into mechanical or electrical power [17, 18]. Theoretically, various model systems performing thermodynamic cycles have been proposed as the quantum heat engines (QHEs), dating back to the three-level masers proposal in 1959 [19]. Recently, more attentions are drawn to the relationship between different types of QHEs [20–23], irreversible work and inner friction [24, 25], the impact of coherence [26–28] and the application prospects and the transition to refrigerators [29–33]. These QHEs not only comply with the classical laws of thermodynamics but also follow the rules of quantum mechanics [34–36]. Consequently, the quantum thermodynamics is boosted by engineering a variety of quantum devices.

Among the QHEs, the quantum Otto heat engine (QOHE), mimicking the common four-strokes car engine, has been extensively studied [37–44]. The working substance is only a quantum harmonic oscillator with a tunable vibration frequency. The heat engine is alternately coupled to a hot and a cold reservoir. The 4-stroke Otto cycle consists of two isochoric processes and two adiabatic

processes. During the isochoric processes, the QOHE exchanges heat with the hot or cold baths but keeps the frequency constant. In the adiabatic processes, the work input or output changes the frequency of the oscillator.

In this paper, we take advantage of the driven-dissipative Schrödinger equation to study the time evolution of the quantum Otto cycle process and evaluate the performance of QOHE. The time-dependent probability distribution of the oscillator's energy levels is calculated by the driven-dissipative Schrödinger equation. The time evolutions of the internal energy, entropy, power and efficiency are simulated. The quantum machine starts from the ground state and the state with equal probability distribution on several lower energy levels, respectively. In the former case, the efficiency and power increase with the number of the Otto cycles until they reach a stable value. In the latter case, the efficiency can be improved beyond the Otto limit, or even the Carnot limit. The overrange is due to the contribution of the energy stored in the initial state. It implies an effective method to enhance the performance of the QOHE. Thus, we suggest that periodically pumping quantum heat engine could raise the efficiency. Furthermore, we propose a possible design of a new quantum engine working in a single bath to convert the pump energy into the mechanical work. Such an engine may be used for working in the microenvironments. We also study the balance between the net power output and the machine efficiency since it is impossible to realize the maximums of both the efficiency and power output at the same time.

## II. MODEL OF QUANTUM OTTO HEAT ENGINE

We apply the driven-dissipative Schrödinger equation [45, 46] to study the time evolution of the QOHE. The energy exchange between the QOHE and the heat reser-

---

\*Electronic address: junchang@snnu.edu.cn

voirs is described by the driven-dissipative operator  $D$ . Previously, we call it the dissipative operator in the decaying process [45, 46]. This equation could deal with strong system-environment coupling and the substantial environmental memory effects, as demonstrated in our previous work [47]. The dissipative Schrödinger equation with the time-dependent quantum state is written as

$$i\hbar \frac{d|\psi(t)\rangle}{dt} = (H_0 + iD)|\psi(t)\rangle, \quad (1)$$

where the Hamiltonian  $H_0$  of the quantum harmonic oscillator with a time-dependent frequency reads

$$H_0 = \hbar\omega a^\dagger a, \quad (2)$$

where  $a^\dagger$  and  $a$  are the Bosonic creation and annihilation operators. Alternatively,

$$H_0 = \sum_n E_n |n\rangle \langle n|, \quad (3)$$

where the energy of the ground state  $|0\rangle$  is assumed to be zero,  $|n\rangle$  is the  $n$ -bosons state of the oscillator, and the corresponding energy  $E_n = n\hbar\omega$ .

The  $D$  operator describes the state changes of the system by surroundings, which is given by

$$D = \frac{\hbar}{2} \sum_n \frac{d \ln P_n(t)}{dt} |n\rangle \langle n|, \quad (4)$$

with the system state  $|\psi(t)\rangle = \sum_n c_n(t) |n\rangle$ .  $P_n(t) = |c_n(t)|^2$  is the occupation probability of the  $n$ -bosons state. The time evolution of the probability distribution function  $P_n(t)$  of the  $n$ th state is described by the rate equation

$$\begin{aligned} \frac{dP_n(t)}{dt} = & -2n\Gamma P_n(t) + 2(n+1)\Gamma P_{n+1}(t) \\ & - 2\Gamma e^{-n\hbar\omega/k_B T} [-nP_{n-1}(t) + (n+1)P_n(t)], \end{aligned} \quad (5)$$

where  $\Gamma$  is the relaxation constant of the oscillator induced by the reservoirs. The factor  $e^{-n\hbar\omega/k_B T}$  is introduced to ensure the rate equation obeying the usual detailed balance relations.

Starting from a given initial population distribution  $P_n(t=0)$ , we solve the driven-dissipative Schrödinger equation and obtain the temporal variation of  $P_n(t)$ . Thus, the time-dependent internal energy of the QOHE reads

$$U(t) = \sum_n E_n P_n(t). \quad (6)$$

The internal energy of the engine may be changed by the work output or input as well as the exchange heat with

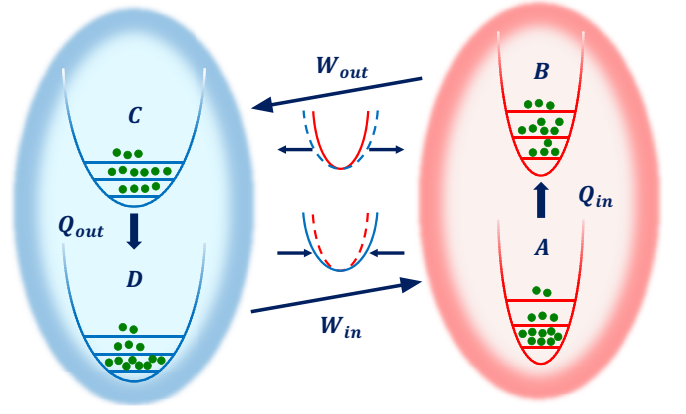


FIG. 1: Schematic cycle of the quantum Otto heat engine mimicking a classical 4-cycle engine. The cycle includes two isochoric processes ( $A \rightarrow B$ ,  $C \rightarrow D$ ) and two adiabatic processes ( $B \rightarrow C$ ,  $D \rightarrow A$ ). In the isochoric phases, the oscillator absorbs the heat  $Q_{in}$  from the hot bath with the temperature  $T_h$  and releases the heat  $Q_{out}$  to the cold bath with the temperature  $T_c$ , respectively. In the adiabatic phases without entropy change, the work output  $W_{out}$  and work input  $W_{in}$  induce the decrease and increase of the oscillator frequency, respectively. The horizontal line segments in the parabolic curves represent the energy levels of the oscillator and the bottom horizontal line indicates the ground state.

a bath. According to the first law of thermodynamics  $dU = dQ + dW$ , then [38, 48]

$$dQ = \sum_n E_n dP_n; \quad dW = \sum_n P_n dE_n. \quad (7)$$

During the thermal cycle, the occupation probability  $P_n$  of the  $n$ -bosons state changes in the endothermic and exothermic processes, and keeps constant in the adiabatic processes. Accordingly, the von Neumann entropy  $S(t)$  as function of occupation distribution  $P_n(t)$  is written as

$$S(t) = -k_B \sum_n P_n(t) \ln P_n(t), \quad (8)$$

where  $k_B$  is the Boltzmann constant.

Let address the 4-stroke Otto cycle in more detail. In the isochoric processes, the heat exchange with the heat reservoirs changes the particle occupation allocation  $P_n(t)$  without work done or  $dW = 0$ , i.e., in the stages  $A \rightarrow B$  and  $C \rightarrow D$ , as shown in Fig. 1. In the adiabatic or isentropic processes, the entropy  $S(t)$  keeps a constant since there is no change of the particle occupation on each level or  $dP_n = 0$ , and no heat exchange with the heat reservoirs or  $dQ = 0$ , i.e., in the stages  $B \rightarrow C$  and  $D \rightarrow A$ .

$A \rightarrow B$ : starting from an initial state at the point  $A$ , the QOHE contacts the hot bath with the temperature  $T_h$ . The oscillator is heated up by the hot bath and keeps its frequency  $\omega_h$  constant. To the point  $B$ , it stops

exchanging heat with the hot bath. The total absorbed heat is

$$Q_{in} = \sum_n n \hbar \omega_h (P_n^B - P_n^A). \quad (9)$$

$B \rightarrow C$ : the machine does work in adiabatic expansion step. The von Neumann entropy remains unchanged,  $dP_n = 0$  or  $P_n^C = P_n^B$ . The oscillation frequency relaxes from  $\omega_h$  to  $\omega_c$ , and the work output is

$$W_{out} = \sum_n n \hbar (\omega_h P_n^B - \omega_c P_n^C). \quad (10)$$

$C \rightarrow D$ : the heat engine couples to the cold bath at the temperature  $T_c$ . The QOHE keeps the same frequency  $\omega_c$  and releases the heat  $Q_{out}$  to the cold bath with

$$Q_{out} = \sum_n n \hbar \omega_c (P_n^C - P_n^D). \quad (11)$$

$D \rightarrow A'$ : the adiabatic compression starts and the frequency of the oscillator is enhanced from  $\omega_c$  to  $\omega_h$  by the input work

$$W_{in} = \sum_n n \hbar (\omega_h P_n^{A'} - \omega_c P_n^D), \quad (12)$$

with  $P_n^{A'} = P_n^D$ . It is worthy of noting that the  $P_n^{A'}$  is not always equal to the  $P_n^A$  unless the Otto cycle is periodically stable.

The effective or net work output  $W_{eff}$  throughout the Otto cycle is given by

$$W_{eff} = W_{out} - W_{in}. \quad (13)$$

Substituting the Eqs. (10) and (12) into Eq. (13), the total effective work  $W_{eff}$  done per Otto cycle is written as

$$W_{eff} = \sum_n n \hbar \left[ (\omega_h P_n^B - \omega_c P_n^C) - (\omega_h P_n^{A'} - \omega_c P_n^D) \right]. \quad (14)$$

Applying the conventional definition, the heat-work conversion efficiency  $\eta$  for the QOHE is given by

$$\eta = \frac{W_{eff}}{Q_{in}}. \quad (15)$$

Combining Eq. (14) and (9), the efficiency  $\eta$  is rewritten as

$$\eta = \frac{\sum_n n \hbar \left[ \omega_h (P_n^B - P_n^{A'}) - \omega_c (P_n^C - P_n^D) \right]}{\sum_n n \hbar \omega_h (P_n^B - P_n^A)}. \quad (16)$$

Without inner friction, one has  $P_n^B = P_n^C$ ,  $P_n^D = P_n^{A'}$ . Then, the efficiency  $\eta$  can be obtained by simplifying Eq. (16) as

$$\eta = \eta_O \frac{\sum_n n (P_n^B - P_n^{A'})}{\sum_n n (P_n^B - P_n^A)}, \quad (17)$$

with the Otto efficiency  $\eta_O = 1 - \omega_c/\omega_h$ .

### III. TIME EVOLUTION OF QUANTUM OTTO HEAT ENGINE

#### A. Otto Cycle without formation of thermal balance

In this section, we simulate the time evolution process of the 4-stroke Otto cycle without formation of thermal balance with the baths. Each period includes four same time segments, e.g.,  $\tau = \tau_{AB} = \tau_{BC} = \tau_{CD} = \tau_{DA}$ .

In all the numerical calculations, we set the lower oscillator energy  $\hbar\omega_c$  as the energy unit, and  $\tau_c = 2\pi/\omega_c$  as the time unit. The relaxation constant between the oscillator and the reservoirs  $\Gamma = 0.1$  in Eq. (5) for the time evolution of the probability distribution function.

During the working stroke, the oscillator frequency reducing or increasing is similar to the volume expanding or compressing in the classical model. We set the time evolution of the frequency function as  $\omega(t) = \omega_{h,c} - t(\omega_{h,c} - \omega_{c,h})/\tau$ . The harmonic frequency gradually decreases from  $\omega_h$  to  $\omega_c$  during the time  $\tau_{BC}$  in the work output stages and gradually increases from  $\omega_c$  to  $\omega_h$  during the time  $\tau_{DA}$  in the work input stages. These working strokes take place under adiabatic conditions, and no heat exchange with heat reservoirs or  $dQ = 0$ . During the thermal exchanging stroke, the vibration frequency is kept constant, and the oscillator exchanges heat with the reservoir without work done or  $dW = 0$ .

The time evolutions of the internal energy  $U$ , entropy  $S$  and efficiency  $\eta$  depend on the time-dependent probabilities of the oscillator's energy levels. The occupancy distribution is determined by solving the driven-dissipative Schrödinger equation.

Firstly, we set the ground state of the oscillator as the initial state. The time evolution of the internal energy  $U$  is shown in Fig. 2(a). The thermal engine reaches cyclostationary state after several periods. With the number  $N$  of the Otto cycle increasing, the quantum machine gradually approaches periodically steady. For instance, the number of particles on each state reach constant values at points  $A, B, C, D$ , as shown the right of the separator in Fig. 2. Since the population of particles on per eigenstate dose not changes during the thermal insulation phases, i.e.,  $dP_n = 0$ , according to Eq. (8), there is no change in the von Neumann entropy  $dS = 0$ , obeying the laws of thermodynamics. In Fig. 2(b), the dash lines depict the constant entropies independent of time. In addition, we obtain the evolutions of efficiency at different working durations  $\tau$  as the illustration in Fig. 3(a). The Otto cycle is not periodic stability in the initial several

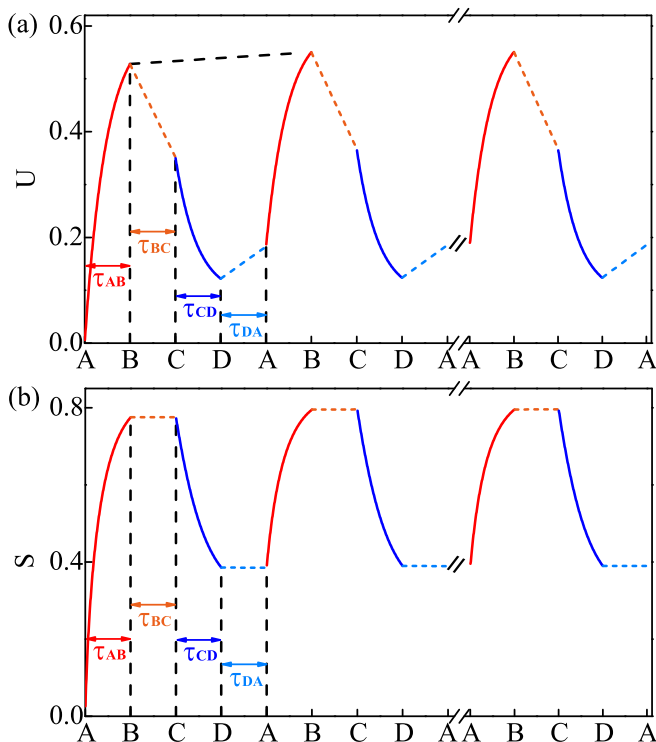


FIG. 2: The time evolutions of (a) the internal energy  $U$  and (b) the entropy  $S$  in the QOHE starting from the ground state to the periodic steady state. The red and blue solid lines indicate the two isochoric processes in the duration  $\tau_{AB}$  and  $\tau_{CD}$ . The orange and light-blue dashed lines indicate the two adiabatic processes with the constant entropies in the segments  $\tau_{BC}$  and  $\tau_{DA}$ . In our numerical calculations, we set  $\hbar\omega_c$  as the unit of energy, and  $\tau_c = 2\pi/\omega_c$  as the unit of time. The working duration  $\tau = 2.0$ . The harmonic oscillators of low frequency  $\hbar\omega_c = 1.0$  and high frequency  $\hbar\omega_h = 1.5$ . The temperature of cold bath  $k_B T_c = 0.4$  and the temperature of the hot bath  $k_B T_h = 1.2$ , respectively. The relaxation constant between the oscillator and the reservoirs  $\Gamma = 0.1$ . The right side of the separator shows the results when the Otto cycle reaches a periodical stable state. The top black oblique dashed line indicates that the difference of the internal energy  $U$  at the points  $B$  and  $B'$  before the machine reaches a stable state.

periodic cycles. The longer the evolution time lasts, the closer  $P_n^A$  is to  $P_n^{A'}$ , which means that the efficiency  $\eta$  is approaching  $\eta_O$ , see Eq. (17). At the same time, the non-steady cycle, the longer the working duration  $\tau$  is, the higher the efficiency  $\eta$  is. Because the QOHE starts from the ground state,  $Q_{in}$  in the first-stroke is much larger than that in subsequent cycles. Consequently, the efficiency is lower than the Otto limit in the first stage. The efficiency  $\eta$  of the QOHE could reach a stable value after several cycles. It is worth noting that  $P_n^{A'} = P_n^A$  holds only when the Otto cycle reaches a steady cyclical state and the efficiency  $\eta$  in Eq. (17) reaches the Otto limit  $\eta_O$ . On the other hand, as long as the probability of  $P_n^A$  is different from  $P_n^{A'}$ , the efficiency deviates from the Otto

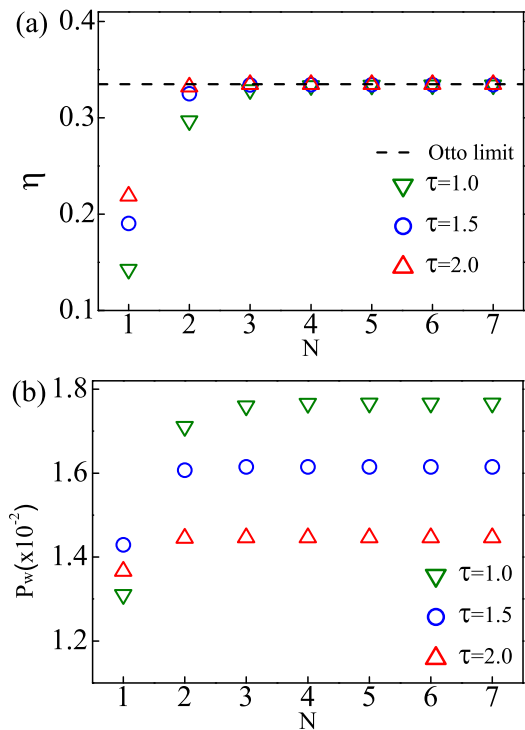


FIG. 3: The efficiency  $\eta$  (a) and power  $P_W$  (b) versus the number  $N$  of the Otto cycles starting from the ground state. The single-segment time  $\tau$  takes 1.0, 1.5 and 2.0. The temperature and frequency parameters are the same as those in Fig. 2. The power is expressed in relative unit of energy and time.

limit  $\eta_O$ .

The power output  $P_W$  is another indicator to judge the performance of the QOHE. It could be expressed as

$$P_W = W_{eff}/4\tau, \quad (18)$$

where  $4\tau$  is total time of a periodic Otto cycle. The time evolution of power is illustrated in Fig. 3(b). During the initial several cycles, the power is lower than the value in the stable cyclic state. The working substance does not warm up to the optimal working order in the beginning few cycles. The power is also lower according to the Eqs. (13) and (18). The power reaches maximum as long as the cycle reaches a fixed periodic state. In addition, the shorter the working cycle duration is, the higher the output power is at the regular stable states, which is similar to that of classic heat engines.

Secondly, we set the initial state with the equal probability distribution on the three lower energy levels of the oscillator. All the other parameters such as the temperatures and frequencies are the same as the previous case. Both the energy and entropy of this initial state is much higher than that in the case starting from the ground state. On account of the speedy redistribution of the probabilities among the high energy levels in the initial stage, the energy quickly decays at the beginning of the evolution and gradually tends to a periodic stabilization,

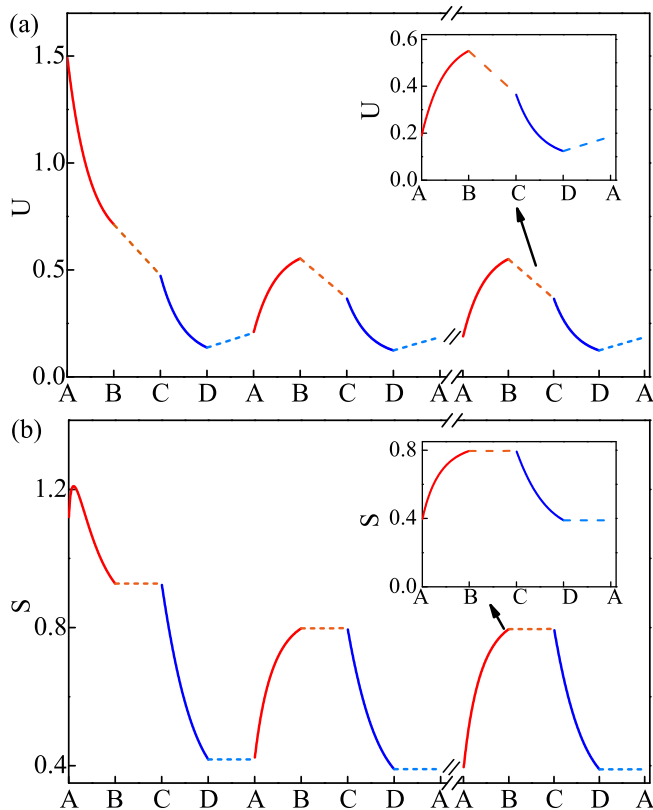


FIG. 4: The time evolutions of the energy  $U$  (a) and entropy  $S$  (b) starting from a initial state with the equal probability distribution on the lower three energy levels. The parameters of temperature  $T_{c,h}$ , frequency  $\omega_{c,h}$  and the duration of single-stroke  $\tau$  are the same as that in previous case starting from the ground state. The red and blue solid lines represent endothermic and exothermic strokes, respectively. The orange and light-blue dashed lines represent the adiabatic working strokes. The enlarged diagram at the right side of the separator indicates that the cycle has reached the periodic state.

as shown in Fig. 4(a). In the starting periods, the energy of the QOHE even releases into the hot bath in the form of heat during the  $\tau_{AB}$  or  $Q_{in} < 0$ . Fig. 4(b) illustrates the temporal evolution of the entropy. The entropy increases at the beginning due to the particle redistributing on more states, and then gradually decreases as particles tending to locate on the lower energy levels during the preliminary period.

Fig. 5(a) shows the time evolution of the efficiency. In the beginning stages, one finds the negative efficiency value due to the negative  $Q_{in}$  and hence negative efficiency  $\eta = W_{eff}/Q_{in}$ . The  $Q_{in}$  gradually approaches zero and then becomes positive. It is worth noting that in the 2nd period, the efficiency even exceeded the Carnot or Otto limit. This does not mean that the thermodynamic laws are violated, and it is attributed to the contribution from the energy stored in the initial state. consequently, it provides a route to improve the efficiency of the QOHE by external control, for example, populat-

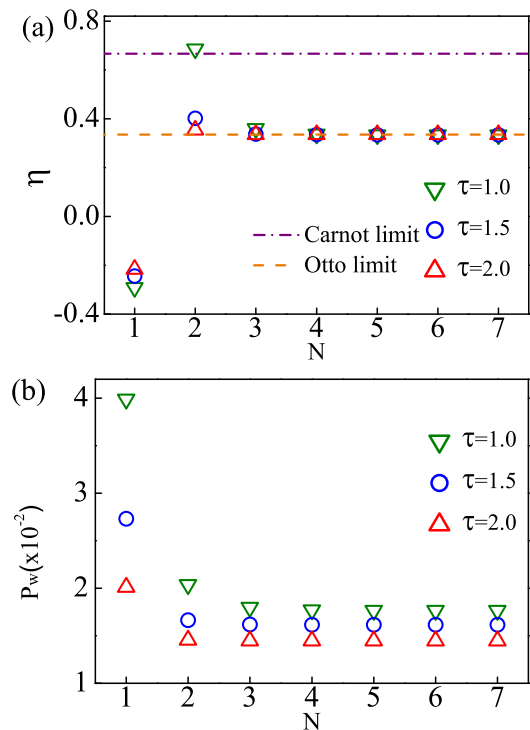


FIG. 5: The efficiency  $\eta$  (a) and power  $P_W$  (b) versus the number of cycles  $N$  with the equal probability distribution on the three lower energy levels as the initial state. The single-segment time  $\tau$  takes different values. The temperature and frequency parameters are the same as those in Fig. 2, respectively.

ing the high levels of the QHE by light or vibration pump. In the stable periodic state of the QOHE, the efficiency returns to the Otto limit  $\eta_O$ . The diagram of power evolution is pictured in Fig. 5(b). The power decays from a higher value to a constant. As the Otto cycle approaches a cyclostationary state, the time evolutions of  $U$ ,  $S$ ,  $\eta$  and  $P_W$  are all the same as those starting from the ground state.

## B. QHE with Single-bath

Heat engine always operates in two heat reservoirs. However, two baths with different temperature are difficult to realize in microenvironments, such as organism and nanostructures. Since the initial state affects the time evolutions of the power, internal energy, entropy and the efficiency at least in the early QHE cycles, we could periodically pump the QHE and improve its performance. Furthermore, here, we propose to pump the quantum engine with a light or vibration pump and convert the pump energy into the mechanical work in a single heat reservoir or in a normal temperature environment. In other words, the energy provided by pump substitutes the heat absorption from the hot bath in the Otto cycles,

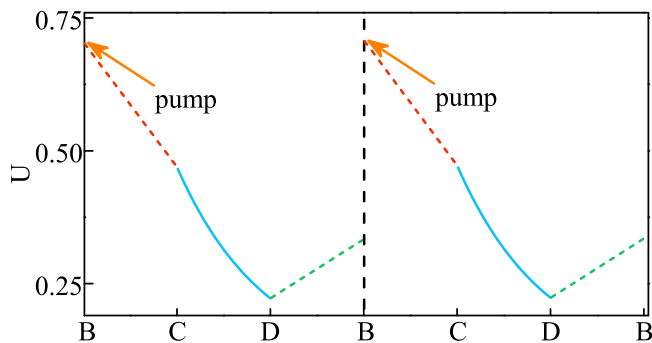


FIG. 6: The time evolution of the energy  $U$  under periodically pumping in a single heat reservoir. Here, single-stage duration  $\tau = 1.0$  and the thermal source at fixed  $k_B T_c = 0.4$ . The frequencies of harmonic oscillators are the same as the previous cases. The red and green dashed lines show the segments of isentropic working; the light-blue solid lines show the segments of isochoric heat release. The pumping operation is performed at the beginning of each cycle as indicated by the orange arrows. The pump duration  $\tau_{AB}$  is ignored for it is much shorter than  $\tau$ .

and then the quantum engine operates in a single heat bath with the temperature  $T_c$ . The engine is regularly pumped at the beginning of the cycles to initialize the occupation probability distribution. Since the pump duration  $\tau_{AB}$  is extremely short, comparing with the time segments of  $\tau_{BC}$ ,  $\tau_{CD}$  and  $\tau_{DB}$ , we neglect  $\tau_{AB}$  in our figures in this model. The evolution process of the internal energy is shown in Fig. 6. The QOHE is periodically pumped from the ground state to the first excited state at beginning of each cycle. This engine actually converts the pump energy into heat and mechanical work. The heat release process is necessary because the pump energy is impossible to be converted into work completely without the heat dissipation according to the second law of thermodynamics. During the adiabatic strokes, the processes of the work input and output are similar to the compression and expansion of classical heat engine. The Otto cycle can be redivided into four processes: pump, expansion, heat release and compression. The efficiency is redefined as the ratio of the net work output to the pump energy. In Fig. 6, the efficiency is 18%.

### C. Otto cycle with thermal balance

We have studied the performance of the QOHE without forming thermal equilibrium with the heat baths in the above sections. In the following, we prolong the duration of periodic cycle to make the machine reach the thermal equilibrium with the baths in the heat exchange processes. The harmonic oscillator's frequency and environmental conditions are exactly the same as those in the previous sections. When the QOHE reaches thermal balance with the heat reservoirs, the population probabilities obey the Boltzmann distribution,  $P_n \propto e^{-E_n/k_B T}$ .

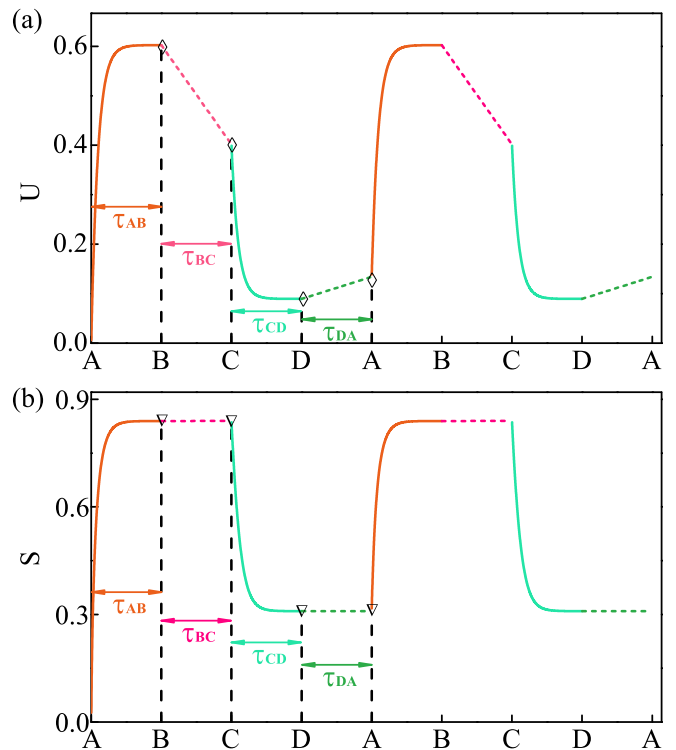


FIG. 7: The time evolutions of the energy  $U$  (a) and entropy  $S$  (b) with the QOHE reaching thermal balance with the baths.  $\hbar\omega_c = 1.0$  and  $\hbar\omega_h = 1.5$ . We set the working time of single-step  $\tau = 10.0$ . The temperature parameters of cold bath and hot bath are  $k_B T_c = 0.4$  and  $k_B T_h = 1.2$ . The pink and green solid lines display the isochoric heat exchange stages; The orange and light-green dashed lines display the isentropic working stages. The hollow diamond and triangle symbols represent analytical results, exactly locating on the numerically calculated curves.

During the heat-exchange processes, the frequencies of the harmonic oscillators remain unchanged. The population distribution function  $P_n$  at the thermal balance could be calculated analytically. Therefore, the analytical value of the internal energy and the entropy at the points  $A$ ,  $B$ ,  $C$ ,  $D$  are labeled on the curves, in good agreement with our numerical calculations, see Fig. 7. The initial state also starts from the ground state, and the cycle reaches stable in the first stage  $\tau_{AB}$ . Only in the first cycle, the absorbed heat and efficiency are different from those in the subsequent cycles.

QHEs often fail to maximize both the output power and the efficiency [4]. The balance between the power and efficiency is pursued. We fix the cold bath temperature a constant value, and adjust the hot bath temperature as well as the frequency ratio  $\omega_c/\omega_h$ . The relationship between the efficiency versus the output power is shown in Fig. 8. The power versus efficiency shows a quasi-parabolic curve. It is impossible for both of them to reach the maximum. The highest efficiency of a QOHE is limited by the Carnot limit  $\eta_C = 1 - T_c/T_h$  [38, 39, 48, 49]

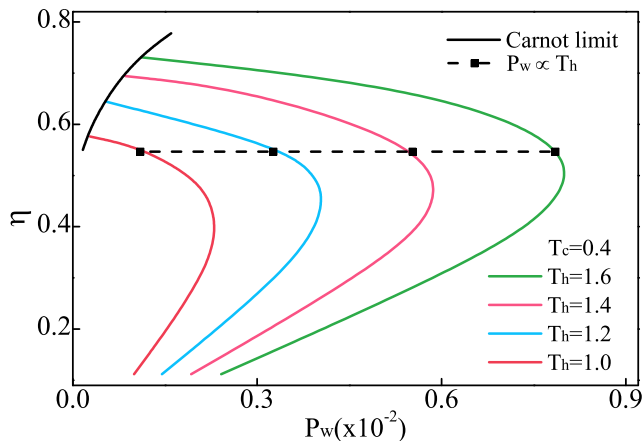


FIG. 8: The efficiency  $\eta$  versus the effective power output  $P_W$  of QOHE. Different colored lines represent the relationship between efficiency and net output power at different  $T_h$  by gradually changing the frequency ratio  $\omega_c/\omega_h$ . The cold bath temperature  $k_B T_c = 0.4$ . The black horizontal dashed line sketches the power  $P_W$  vs  $T_h$  at a fixed  $\eta$ . Black solid line indicates the Carnot limit, constraining the efficiency of the QOHE.

with the ratio  $\omega_c/\omega_h = T_c/T_h$ . For the same efficiency, the higher temperature of the hot bath leads to the higher output power, as shown by the black dashed line in Fig. 8. At the fixed temperature ratio  $T_h/T_c$ , the efficiency could be improved with the frequency ratio  $\omega_h/\omega_c$  enhancement until it reaches Carnot limit.

## IV. CONCLUSION

To conclude, we have probed the time evolution of the quantum Otto cycle process and the performance of the QOHE with a single oscillator as the working substance. We calculated the time-dependent population distribution of the oscillator's energy levels by solving the driven-dissipative Schrödinger equation and simulated the time evolutions of the internal energy, entropy, power and efficiency. We show that the different initial states have different impacts on these quantities in the transient period before the Otto cycle becomes periodical stable. In the transition time, the efficiency and power differs from the corresponding values in the stable Otto cycles. The efficiency even surpasses the Otto limit and the Carnot limit, which is attributed to the contribution from the energy stored in the initial state. Therefore, we suggest that the periodically pumping could raise the efficiency of the quantum machine. Furthermore, we propose a novel quantum engine in ambient condition to convert the pump energy into the mechanical work. Such an engine could work in the microenvironments without a large temperature difference, such as biological tissues in vivo. We expect that the operational protocol presented here is applied to modeling a quantum engine with the advantage of controllability.

*Acknowledgments.*—We are thankful to Jize Zhao for fruitful discussions. This work is supported by the National Natural Science Foundation of China No.91750111.

- 
- [1] P. Hänggi and F. Marchesoni, *Rev. Mod. Phys.* **81**, 387 (2009).
- [2] B. Lin and J. Chen, *Phys. Rev. E* **67**, 046105 (2003).
- [3] J.-P. Brantut, C. Grenier, J. Meineke, D. Stadler, S. Krinner, C. Kollath, T. Esslinger, and A. Georges, *Science (New York, N.Y.)* **342**, 713 (2013).
- [4] O. Abah, J. Roßnagel, G. Jacob, S. Deffner, F. Schmidt-Kaler, K. Singer, and E. Lutz, *Phys. Rev. Lett.* **109**, 203006 (2012).
- [5] J. V. Koski, V. F. Maisi, J. P. Pekola, and D. V. Averin, *Proc. Natl. Acad. Sci.* **111**, 13786 (2014).
- [6] S. Rana, P. S. Pal, A. Saha, and A. M. Jayannavar, *Phys. Rev. E* **90**, 042146 (2014).
- [7] J. Roßnagel, S. T. Dawkins, K. N. Tolazzi, O. Abah, and K. Singer, *Science* **352**, 325 (2016).
- [8] D. von Lindenfels, O. Gräß, C. T. Schmiegelow, V. Kaushal, J. Schulz, M. T. Mitchison, J. Goold, F. Schmidt-Kaler, and U. G. Poschinger, *Phys. Rev. Lett.* **123**, 080602 (2019).
- [9] A. E. Hill, Y. V. Rostovtsev, and M. O. Scully, *Phys. Rev. A* **72**, 043802 (2005).
- [10] W. Hübner, G. Lefkidis, C. D. Dong, D. Chaudhuri, L. Chotorlishvili, and J. Berakdar, *Phys. Rev. B* **90**, 024401 (2014).
- [11] E. Geva and R. Kosloff, *J. Chem. Phys.* **96**, 3054 (1992).
- [12] G. Thomas and R. S. Johal, *Phys. Rev. E* **83**, 031135 (2011).
- [13] J. P. S. Peterson, T. B. Batalhão, M. Herrera, A. M. Souza, R. S. Sarthour, I. S. Oliveira, and R. M. Serra, *Phys. Rev. Lett.* **123**, 240601 (2019).
- [14] N. Linden, S. Popescu, and P. Skrzypczyk, *Phys. Rev. Lett.* **105**, 130401 (2010).
- [15] N. Brunner, N. Linden, S. Popescu, and P. Skrzypczyk, *Phys. Rev. E* **85**, 051117 (2012).
- [16] J. B. Brask, G. Haack, N. Brunner, and M. Huber, *New J. Phys.* **17**, 113029 (2015).
- [17] G. Benenti, G. Casati, K. Saito, and R. S. Whitney, *Phys. Rep.* **694**, 1 (2017).
- [18] J. Klaers, S. Faelt, A. Imamoglu, and E. Togan, *Phys. Rev. X* **7**, 031044 (2017).
- [19] H. E. D. Scovil and E. O. Schulz-DuBois, *Phys. Rev. Lett.* **2**, 262 (1959).
- [20] H. T. Quan, Y. X. Liu, C. P. Sun, and F. Nori, *Phys. Rev. E* **76**, 031105 (2007).
- [21] R. Uzdin, A. Levy, and R. Kosloff, *Phys. Rev. X* **5**, 031044 (2015).
- [22] C. Elouard, D. Herrera-Martí, B. Huard, and A. Auffèves, *Phys. Rev. Lett.* **118**, 260603 (2017).
- [23] J. Klatzow, J. N. Becker, P. M. Ledingham, C. Weinzetl, K. T. Kaczmarek, D. J. Saunders, J. Nunn, I. A. Walmsley, R. Uzdin, and E. Poem, *Phys. Rev. Lett.* **122**, 110601 (2019).

- [24] Y. Rezek and R. Kosloff, *New J. Phys.* **8**, 83 (2006).
- [25] F. Plastina, A. Alecce, T. J. G. Apollaro, G. Falcone, G. Francica, F. Galve, N. Lo Gullo, and R. Zambrini, *Phys. Rev. Lett.* **113**, 260601 (2014).
- [26] M. O. Scully, M. S. Zubairy, G. S. Agarwal, and H. Walther, *Science* **299**, 862 (2003).
- [27] S. Rahav, U. Harbola, and S. Mukamel, *Phys. Rev. A* **86**, 043843 (2012).
- [28] H. P. Goswami and U. Harbola, *Phys. Rev. A* **88**, 013842 (2013).
- [29] D. Gelbwaser-Klimovsky, R. Alicki, and G. Kurizki, *Phys. Rev. E* **87**, 012140 (2013).
- [30] R. Kosloff and A. Levy, *Annu. Rev. Phys. Chem.* **65**, 365 (2014).
- [31] R. Uzdin and R. Kosloff, *New J. Phys.* **16**, 095003 (2014).
- [32] P. P. Hofer, M. Perarnau-Llobet, J. B. Brask, R. Silva, M. Huber, and N. Brunner, *Phys. Rev. B* **94**, 235420 (2016).
- [33] P. A. Camati, J. F. G. Santos, and R. M. Serra, *Phys. Rev. A* **102**, 012217 (2020).
- [34] H. T. Quan, P. Zhang, and C. P. Sun, *Phys. Rev. E* **72**, 056110 (2005).
- [35] R. Kosloff, *Entropy* **15**, 2100 (2013).
- [36] P. Skrzypczyk, A. J. Short, and S. Popescu, *Nat. Commun.* **5**, 4185 (2014).
- [37] T. Feldmann and R. Kosloff, *Phys. Rev. E* **68**, 016101 (2003).
- [38] T. D. Kieu, *Phys. Rev. Lett.* **93**, 140403 (2004).
- [39] J. Roßnagel, O. Abah, F. Schmidt-Kaler, K. Singer, and E. Lutz, *Phys. Rev. Lett.* **112**, 030602 (2014).
- [40] R. Kosloff and Y. Rezek, *Entropy* **19**, 136 (2017).
- [41] G. Watanabe, B. P. Venkatesh, P. Talkner, and A. del Campo, *Phys. Rev. Lett.* **118**, 050601 (2017).
- [42] P. A. Camati, J. F. G. Santos, and R. M. Serra, *Phys. Rev. A* **99**, 062103 (2019).
- [43] A. Das and V. Mukherjee, *Phys. Rev. Research* **2**, 033083 (2020).
- [44] M. Wiedmann, J. T. Stockburger, and J. Ankerhold, *New J. Phys.* **22**, 033007 (2020).
- [45] J. Chang, A. J. Fedro, and M. van Veenendaal, *Phys. Rev. B* **82**, 075124 (2010).
- [46] M. van Veenendaal, J. Chang, and A. J. Fedro, *Phys. Rev. Lett.* **104**, 067401 (2010).
- [47] J. Chang, A. Fedro, and M. van Veenendaal, *Chem. Phys.* **407**, 65 (2012).
- [48] T. D. Kieu, *Eur. Phys. J. D.* **39**, 115 (2006).
- [49] J.-M. Park, S. Lee, H.-M. Chun, and J. D. Noh, *Phys. Rev. E* **100**, 012148 (2019).